Drug-induced symmetry effects on ventricular repolarization dynamics

Pablo Daniel Cruces [a,b,*], Alejandra Toscano [a], Francisco Javier Alvarado Rodríguez [c,d], Rebeca Romo-Vázquez [d], Pedro David Arini [a,b]

[a] Instituto de Ingeniería Biomédica, UBA, Paseo Colón 850 (C1063ACV), Buenos Aires, Argentina
[b] Instituto Argentino de Matemática 'Alberto P. Calderón', CONICET, Saavedra 15 (C1083ACA), Buenos Aires, Argentina
[c] Departamento de Electromecánica, Universidad Autónoma de Guadalajara, Jalisco, Mexico
[d] Departamento de Bioingeniería Traslacional, CUCEI, Universidad de Guadalajara, Mexico

ARTICLE INFO

Keywords:
Torsade de Pointes
Quaternion
Angular velocity
Vectorcardiogram

ABSTRACT

The detection of proarrhythmic effects of many current drugs has prompted the search for complementary non-invasive markers of cardiotoxicity risk. Indices based on studies of cardiac vector dynamics have emerged. We use quaternions to quantify symmetry changes in cardiac vector velocity during ventricular repolarization, which could signal the arrhythmia risk. Principal component analysis is used to homogenize the information and reduce the space to three dimensions. A comparison with the ratio of normalized areas of the repolarization loop (T-wave) and two standard measurements was made: QT and T peak-end intervals. Assessment was conducted by comparing 52 healthy subjects with patients undergoing treatment with Sotalol: 7 recordings with Torsade de Pointes events and 15 without arrhythmic effects. Significant differences ($p < 5E\text{-}4$) were found in both phases of repolarization in terms of absolute velocities and areas. The ratio between the maximums of each parameter in both halves of the T-wave showed a trend towards 1 in the proximity of an arrhythmic event. Angular velocity ratios reached a sensitivity/specificity pair of 100 (95%CI: 59–100)/90 (95%CI: 79–97) with an AUC of 98.6 (95%CI: 95.7–100) in the comparison of healthy population with at-risk patients. Linear discriminant analysis improved the classification by reaching sensitivity and specificity values of 100 (95%CI: 59–100) and 96 (5%CI: 87–100), respectively. The high performance of the method exceeded the diagnostic power of standard measurements, thus showing its potential to contribute to drug evaluation methods. Further research with a larger number of events is required to generalize the method.

1. Introduction

In view of the increased prescription of medicines and rising rates of deaths globally due to cardiovascular diseases [1], the study of proarrhythmic side effects has moved to the forefront of scientific research and the pharmacological industry. A significant incidence of Torsade de Pointes (TdP) episodes has been observed [2,3] with antiarrhythmic and other non-cardiac drugs, such as antidiuretics, antibiotics, and antidepressants. TdP is a polymorphic ventricular arrhythmia that can be fatal. Figs. 1a and 1b show a normal surface electrocardiogram (ECG) signal and the spontaneous development of a TdP episode respectively.

Currently, the proarrhythmic risk assessment of a drug is determined mainly by measuring the prolongation of the QT interval in ECG [4,5], corrected for heart rate value (QTc), which represents the total time of ventricular depolarization and repolarization (See Fig. 1a). The action of drugs on the ionic currents that underlie action potentials increases the QTc interval. An excessive increase is a sign of cardiac risk [6]. Proarrhythmic effects have recently been observed in drugs that do not prolong the QTc interval [7]. Moreover, some drugs prolong the QTc interval but without reports of adverse effects on the heart [8,9]. For these reasons, several international agencies are supporting the search for independent complementary markers that can aid in developing safer drugs [3].

Since the increase in ventricular repolarization dispersion is recognized as a risk factor for arrhythmias [10], various non-invasive markers of dispersion have been proposed to characterize the effect of multiple drugs as supplementary indices to QTc. Measurements of early and late ventricular repolarization phases have produced significant results, such as Tpe and JTp [11]; two measures of the duration of T-wave phases that have shown distinct responses to drugs that block the hERG potassium channel from those with multichannel action. Other duration measures, such as the 30% drop in both halves of the T-wave, have been proposed as alternative markers [12]. Observations show that the areas associated with these periods may be useful for computing morphology-based biomarkers [13,14]. All these markers

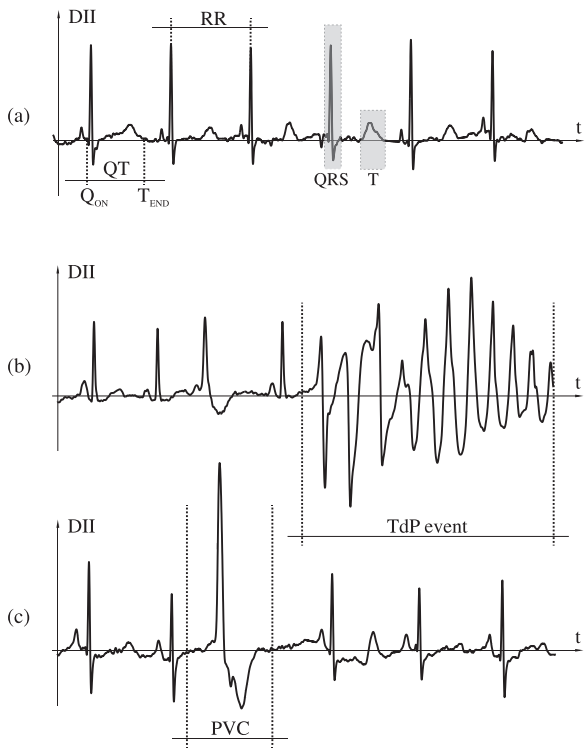

Fig. 1. (a) Normal ECG signal observed on the DII lead. The difference between the Q_{ON} and T_{END} points determines the standard QT index. RR represents the reciprocal of the heart rate; (b) occurrence of a Torsade de Pointes event in a subject in the study population; (c) premature ventricular contraction during T-wave.

provide additional information on QT but depend on the accurate detection of ECG fiducial points. Determining the end and onset of both T-wave and QRS complex with low uncertainty remains a challenge for research, especially when recordings are noisy or pathological.

Observations also show that the increase in T-wave symmetry is associated with an increase in ventricular repolarization dispersion [15]. Subsequent studies have attempted to quantify symmetry features using the ratio of the biomarkers described above [16,10]. In our work, we assessed the symmetry concept from the perspective of the new dynamic markers associated with the cardiac electrical vector and its velocities. This approach, developed from quaternion algebra, proved to be highly effective in recent works on drug effects in both an isolated rabbit heart model [17] and human at-risk patients with a history of arrhythmia [13]. Herein, our aim was to evaluate the efficacy in risk prediction of the ratio of dynamic markers prior to TdP triggering in patients undergoing Sotalol treatment, a well-known drug with proarrhythmic potential. We focused on ventricular repolarization since increased dispersion and premature ventricular contractions (see Fig. 1c) have been associated with the risk of arrhythmias [18,19]. We are confident that our results can contribute to the development of safe drug therapies.

2. Materials and methods

2.1. Dataset

The analysis was based on three study populations.

2.1.1. Torsades de pointes events recorded

This database provided the target population. It was obtained through a project with the Telemetric and Holter ECG Warehouse (THEW) [20] and includes Holter records (long-term ECG) from six patients (48 ± 25 y.o., 3 male and 3 female) who had experienced events of TdP during recording. One patient had two recorded events, so a total of 7 events were captured in the database. Those patients were enrolled in a diagnostic test based on dl-sotalol IV (at 2 mg/kg of body weight in 50 ml of 0.9% saline solution). The test was designed to reveal latent repolarization abnormalities. The TdP events are marked. Four patients had a history of drug-induced TdP (sotalol, amiodarone, amantadine) while the others had antecedents of congenital TdP tendencies. Each recording consisted of 8-lead ECG signals at Fs 180 Hz and 16 bits of resolution.

2.1.2. Sotalol IV and history of TdPs

This population consisted of 15 patients (58 ± 12 y.o., females: 70%) with documented TdP in the context of the use of a drug with QT-prolonging potential: sotalol, sumatriptan, amiodarone, bisacodyl, cipramil, furosemide, clarithromycin, erythromycin, or roxithromycin [21]. Those patients received a dose of sotalol to evaluate individual levels of repolarization reserve. The drug was administered under continuous monitoring in an intensive care unit. Continuous surface ECG recordings were acquired at rest from injection to peak drug concentration. Each recording included 12-lead ECG at 1 kHz of Fs and 5 μV resolution. Although these patients received the same dose as those in the first database, none experienced a TdP event during the challenge and none carried a mutation linked to the major congenital forms of the LQTS.

2.1.3. Physikalisch - Technische Bundesanstalt

From this dataset, we selected all recordings from 52 volunteers (43 ± 15 y.o., females: 25%) with no previous cardiovascular diseases [22,23]. The database was acquired from the Department of Cardiology of the Benjamin Franklin University Clinic in Berlin, Germany, and has been provided to the users of PhysioNet. Each recording includes 15 simultaneously measured signals: the 12 standard ECG leads plus the 3 orthogonal Frank leads. Each signal was digitized at Fs 1 kHz and 16 bits of amplitude resolution.

2.2. Preprocessing

Since the TdP events occurred at different times of the day in each Holter recording (Section 2.1.1), we selected a recording segment of 1 h before the arrhythmic event. The signals in this dataset were resampled to 1 kHz so all the datasets have the same frequency. This does not affect the velocity computations since quaternion methods ensure velocity parameters with a strong correlation (>98%) between 180 Hz and 1000 Hz [24]. For each ECG lead an 80 Hz Butterworth low-pass filter was applied to remove high frequency noise. In addition, a 0.5 Hz Butterworth high-pass filter was applied for baseline wander correction. Both were 5th order and bidirectional to avoid phase distortion. All QRS complexes were delineated automatically using a wavelet-transform based method [25]. If a premature ventricular contraction (PVC) appeared in a recording, the QRS fiducial point was eliminated. PVCs are easily detectable because they are manifested as large amplitude deflections during ventricular repolarization (See Fig. 1c). Their appearance is usually linked to increased ventricular repolarization dispersion and the risk – as in this case – of an arrhythmic event [18,19].

2.3. Segmentation

To construct the time series of the first dataset, a single T-wave from an averaged beat was obtained for each minute throughout the hour before the arrhythmic event experienced by each patient. Ten consecutive beats were taken throughout each minute requiring a correlation greater than 0.9 among the ten QRS complexes ($Q\widehat{R}S \pm 60$ ms). The correlation coefficient was calculated in all leads for each pair of complexes, choosing the lowest correlation value obtained as the final one, such that two QRS complexes would have a correlation > 0.9 as

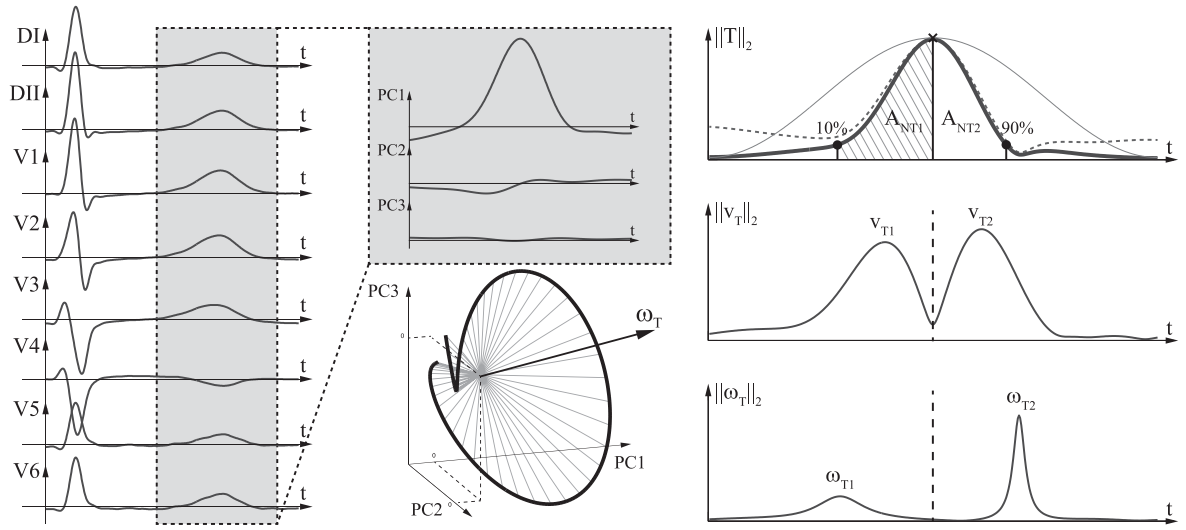

Fig. 2. Decomposition into three principal components (PC) of a T-wave from eight independent leads. The maximum of the 2-norm of the components is computed to separate the halves of the T-wave. The angular (ω_T) and linear (v_T) velocity vectors and their maximums in each half are computed from the three-dimensional signal. The area of each half of the T-wave is obtained after applying a Hamming window (thin line) to the signal (dotted line). The bold line shows a windowed signal.

long as this is true for all leads. The T-waves were obtained in all the samples from $Q\widehat{R}S_i + 60$ ms (T_{ON}) to $Q\widehat{R}S_{i+1} - 150$ ms (T_{END}) for each ith beat of the ten. The accuracy of T_{ON} and T_{END} is not crucial because the maximum velocities do not depend on the exact value of these points. This issue is discussed further below. Every averaged T-wave was obtained in this way and the noise was reduced by applying a 10 Hz Butterworth low-pass filter to each one.

2.4. Principal component analysis

The study of the angular velocity of the cardiac electrical vector requires a three-dimensional space that can usually be obtained directly from the vectorcardiograms [26] or indirectly from an inverse transformation of the ECG such as the Kors matrix [27]. Since the present work analyses a series of recordings from three databases with distinct acquisition methods, principal component analysis (PCA) is an adequate way to homogenize the information and at the same time, reduce it to three orthogonal axes. These axes do not have the same directions of Frank vectorcardiographic (VCG) system. However, the shape of the T-wave loop obtained after transformation should result in a signal with minor differences from that of VCG. Consequently, the 2-norm of the velocities should not have appreciable differences. From each matrix $A_{\text{T-WAVE}}$ (signal from T_{ON} to T_{END}) with the eight independent ECG leads (I, II, V1–V6) and N samples, a Singular Value Decomposition were computed for each averaged T-wave,

$$A_{\text{T-WAVE}} = USV^T \tag{1}$$

where U is an 8×8 matrix, V is NxN and the eight singular values are in the primary diagonal of the $8xN$ matrix S. The first three quantify the energy of the so-called dipolar components of the $\vec{T}_{\text{3-D}}$ signal. The other five singular values represent the non-dipolar components of the T-wave and are not considered in the present analysis. Finally, the decomposed signal D_S appears as follows:

$$D_{S(8\times N)} = S_{(8\times 8)}V^T_{(N\times 8)} \rightarrow \vec{T}_{\text{3-D}} = D_{S(3\times N)} \tag{2}$$

Fig. 2 shows a three-dimensional T-wave that results from the decomposition.

2.5. Dynamic features

The cardiac electrical vector is the signal that results from all the action potentials at every instant in the heart. It is sampled at a frequency Fs. For the nth sample of $\vec{T}_{\text{3-D}}$, the sequence $\vec{T}_{\vec{n}}$ forms the three orthogonal components in the space obtained from PCA during the repolarization process.

2.5.1. Cardiac vector velocity

The linear velocity of the cardiac vector can be obtained by direct differentiation of the signal.

$$\overrightarrow{v_T} = (\vec{T}_{\vec{n}+\vec{1}} - \vec{T}_{\vec{n}}) \cdot Fs \tag{3}$$

As Fig. 2 shows, the 2-norm of the resulting vector has its maximums at the maximum slopes of the ascending and descending T-wave. Meanwhile, the angular velocity $\overrightarrow{\omega}$ is a three-dimensional vector orthogonal to the rotation of the cardiac vector and $\|\overrightarrow{\omega}\|_2$ represents the speed in each sample. Using quaternion algebra makes it possible to avoid the difficulties involved in obtaining this using traditional methods, like Euler matrices. The main advantages involve computation speed and the propagation of uncertainties [28]. Thus, a quaternion $\vec{q}_{\vec{n}}$ was built for each nth sample of $\vec{T}_{\text{3-D}}$.

$$\vec{q}_{\vec{n}} = \frac{(0, \vec{T}_{\vec{n}})}{\left\|\vec{T}_{\vec{n}}\right\|} \tag{4}$$

Then, using the temporal differentiation of $\vec{q}_{\vec{n}}$, we found

$$\dot{\vec{q}}_n = (\vec{q}_{\vec{n}+\vec{1}} - \vec{q}_{\vec{n}}) \cdot Fs \tag{5}$$

The angular velocity was obtained from the imaginary part of the Poisson formula [29]:

$$\overrightarrow{\omega_T} = \dot{\vec{q}}_n \times \bar{\vec{q}}_n \tag{6}$$

In Eqs. (5) and (6), $\bar{\vec{q}}_n$ indicates the quaternion conjugate and the '$\times$' symbol refers to the Hamilton multiplication rule which follows the fundamental formula of quaternions; that is: $i^2 = j^2 = k^2 = ijk = -1$.

Finally, to analyze the T-wave symmetry, the maximum linear and angular velocities in each half were obtained as:

$$\begin{cases} v_{T1} = max(\|\vec{v}(T_{\text{ON}} : T_{\text{PEAK}})\|_2) \\ v_{T2} = max(\|\vec{v}(T_{\text{PEAK}} : T_{\text{END}})\|_2) \\ \omega_{T1} = max(\|\vec{\omega}(T_{\text{ON}} : T_{\text{PEAK}})\|_2) \\ \omega_{T2} = max(\|\vec{\omega}(T_{\text{PEAK}} : T_{\text{END}})\|_2) \end{cases} \tag{7}$$

where T_{PEAK} is obtained from $max(\left\|\vec{T}_{\text{3-D}}\right\|_2)$ (see Fig. 2). The ratios between their both maximums represent the proposed velocity symmetry markers: $\omega_{T21} = \omega_{T2}/\omega_{T1}$ and $v_{T21} = v_{T2}/v_{T1}$.

Table 1
Standard diagnostic with QT_c interval index.

Diagnosis	Young (≤15 y.o.)	Adults	
		Male	Female
Normal	$QT_c < 440$	$QT_c < 430$	$QT_c < 450$
Borderline	440–460	430–450	450–470
Prolonged	$QT_c > 460$	$QT_c > 450$	$QT_c > 470$

2.5.2. T-wave area

We computed the areas of the first (A_{T1}) and second (A_{T2}) halves of the T-wave as common ECG morphological indices for describing drug-induced changes [30,16]. This has been employed as the usual measure in precordial-lead V5 because of its stable repolarization signal. The ratio of the two areas represents another measure of symmetry ($A_{T12} = A_{T1}/A_{T2}$). We also computed the normalized areas of both halves of the T-wave, from 2-norm of the $\vec{T}_{3\text{-D}}$ signal obtained by PCA. The T-wave peak that divides the two halves is obtained as the maximum of the absolute signal. We then applied a Hamming window to taper the extremes of the wave to zero (Fig. 2). We then proceeded to obtain the area from the peak to 10% amplitude in the first (A_{NT1}) and second half (A_{NT2}). The ratio $A_{NT21} = A_{NT2}/A_{NT1}$ defines the symmetry marker of this area.

2.6. Population analysis

The methodology described above was developed to characterize the symmetry of dynamic features one hour before the arrhythmic event experienced by patients in the Torsades de Pointes events recorded database (Section 2.1.1). In the next step, we sought to distinguish this risk population (+TdP) from healthy volunteers (Hs, Section 2.1.3) or other patients who received the same treatment but did not suffer TdP events (−TdP, Section 2.1.2). The values of ω, υ and the areas were obtained for both complementary populations in the first 10 consecutive beats of each recording that reached a correlation greater than 0.9 among the QRS complexes. A two-sided Wilcoxon signed rank test was performed to obtain a significance value (p) for the group means. To obtain decision boundaries to help define symmetry values associated with risk zones, we applied linear discriminant analysis combining no more than two significant features. To achieve greater accuracy for these boundaries, expanded five-dimensional quadratic polynomial spaces were used; such that if A and B are the two selected features, the decision boundary is computed by the linear combination of A, B, $A.B$, A^2 and B^2.

2.7. Standard measurement

Finally, in order to make a comparison with the current standard measure, the QT interval was obtained with the correction of the heart rate using the Bazett formula [6], as:

$$QT_c = \frac{T_{\text{END}} - Q_{\text{ON}}}{\sqrt{RR}} \tag{8}$$

where T_{END} is the end point of ventricular repolarization (T-wave) and Q_{ON} the point of the depolarization onset (QRS complex). Both marks are obtained using a wavelet delineation method [25]. RR is the reciprocal of heart rate (See Fig. 1). Standard diagnoses were made according to Table 1 [6]. We included the computation of Tpe ($T_{\text{END}} - T_{\text{PEAK}}$) for between-populations comparisons. Prolonged TpTe is defined as >85 ms [31].

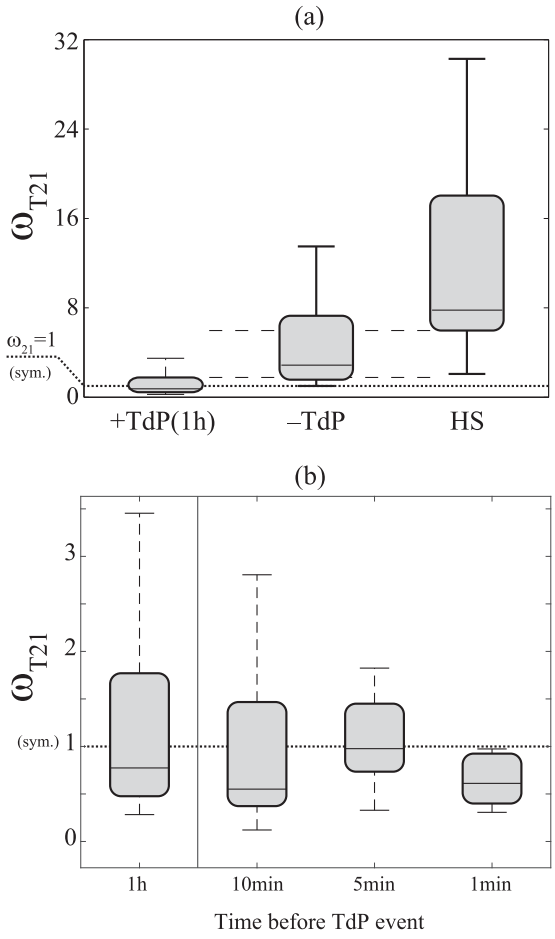

Fig. 3. Angular velocity ratio: (a) Differences between: at-risk patients (+TdP), subjects under the same treatment who did not suffer arrhythmia (−TdP), and healthy subjects (Hs); (b) Temporal evolution of the symmetry index prior to the TdP event.

3. Results

Table 2 lists the mean and standard deviation values of ω, υ and both standard and normalized areas for the ascending and descending limbs of the T-wave. The QTc and Tpe measurements are also shown. Symmetry indices showed statistically significant differences between healthy subjects (HS) and the at-risk population (+TdP) one hour before the TdP episodes with p<5E−4. The ratio of linear velocity υ_{21} also showed differences between the +TdP and −TdP populations.

The symmetry index most notably affected was angular velocity. The trend observed in the at-risk population indicates that the maximum angular velocity of the second half of the T-wave decreased markedly one hour before the TdP event. Therefore, the ratio between the two angular parameters (ω_{T21}) was analyzed and compared to the values for the other populations. This enhanced the differences between the healthy population and the at-risk populations by reaching a p-value of less than 5E-5. In addition, the differences between +TdP and the subjects who, while under the same treatment, did not suffer arrhythmia (−TdP) also increased. Fig. 3a shows a box and whiskers diagram that compares this ratio for the three populations. ω_{T21} reached a sensitivity/specificity pair of 100 (95%CI: 59–100) / 90 (95%CI: 79–97) with an AUC of 98.6 (95%CI: 95.7–100) on its own in the comparison of the healthy population to the at-risk patients. Meanwhile, the standard QT_c index was unable to differentiate the +TdP and −TdP populations, as it reached a pair of 67/85 between +TdP and Hs. Regarding the Tpe interval, although an increase in the

Table 2
Mean (μ) and standard deviation (σ) of new dynamics and standard indices in each half of the T-wave and its ratio. They are reported for the three populations.

Index	HS	−TdP	+TdP (1 h)
	$\mu \pm \sigma$	$\mu \pm \sigma$	$\mu \pm \sigma$
ω_{T1} [rad/s]	30.41 ± 32.88	25.33 ± 18.00	24.74 ± 10.64
ω_{T2} [rad/s]	300.72 ± 204.86	46.05 ± 56.16[a]	26.27 ± 23.08[c]
ω_{T21} [n.u.]	13.05 ± 9.91	3.24 ± 4.71[a]	1.24 ± 1.13[c]
v_{T1} [mV/s]	13.21 ± 4.45	9.13 ± 5.28[a]	8.40 ± 3.49[c]
v_{T2} [mV/s]	18.58 ± 7.71	12.73 ± 6.32[a]	9.66 ± 6.09[c]
v_{T21} [n.u.]	1.43 ± 0.21	1.49 ± 0.44	1.09 ± 0.34[bc]
A_{T1} [μV.ms]	33706.96 ± 17151.11	49972.43 ± 30493.98	28151.32 ± 17770.59
A_{T2} [μV.ms]	18925.16 ± 9890.96	32755.75 ± 17321.82[a]	20019.35 ± 11501.54
A_{T21} [n.u.]	2.31 ± 2.69	1.60 ± 0.79	1.40 ± 0.43[c]
A_{NT1} [μV.ms]	50752.56 ± 22337.35	34980.88 ± 20199.86[a]	23054.38 ± 17984.04[c]
A_{NT2} [μV.ms]	40008.07 ± 17247.43	22149.43 ± 13878.16[a]	20322.41 ± 15518.53[c]
A_{NT21} [n.u.]	1.28 ± 0.17	1.68 ± 0.59[a]	1.22 ± 0.37
QT_C [ms]	433.3 ± 28.9	496.89 ± 34.30[a]	512.74 ± 71.65[c]
Tpe [ms]	74.9 ± 12.0	92.1 ± 29.8	97.1 ± 18.6

[a] −TdP and HS populations.
[b] +TdP and −TdP.
[c] +TdP and HS. +TdP refers to a mean beat 1 h prior the TdP event.

+TdP and −TdP datasets was observed in the comparison to the healthy subjects, no significant differences were found between the populations.

In addition, ω_{T21} was analyzed in time for the +TdP population. The tendency towards symmetry is even more evident as the event approaches, where $\omega_{T21} \to 1$ (See Fig. 3b), as, at one minute prior the arrhythmic event, the at-risk population was completely differentiated from the other two. The normalized areas showed greater significance values than the standard since they were less affected by noise. Regarding the ratios, similar results were reached. The symmetry between the maximum linear velocities was the only index that showed significant differences between the (−TdP) and (+TdP) populations.

Finally, using linear discriminant analysis, we combined the symmetry indices to define risk zones, as shown in Fig. 4. The combination was assessed in the signals one hour before the event since the aim was to obtain an early observation of the risk. With the decision boundaries obtained, the combination of linear and angular velocities reached a sensitivity/specificity pair of 100 (95%CI: 59–100) / 96 (95%CI: 87–100) to differentiate +TdP from Hs, and of 60 (95%CI: 33–84) / 94 (95%CI: 84–99) for −TdP and Hs. The combination of angular velocity with normalized areas improved the efficiency in separating the −TdP and Hs populations, reaching a pair of 80 (95%CI: 52–96) / 98 (95%CI: 90–100).

4. Discussion

Recently, the indices that characterize the dynamics of the cardiac electrical vector have shown great potential as risk markers in cases of acute coronary syndrome [24,32] and drug-induced arrhythmias [17]. Obtaining the angular velocity from quaternions overcomes the difficulty encountered in traditional methods regarding the generation of ill-conditioned matrices and the propagation of numerical uncertainties [28]. In the present study, the maximum angular velocities were combined with linear velocity and T-wave area during ventricular repolarization and studied for the first time in recordings that capture episodes of TdP in patients undergoing Sotalol treatment.

The T-wave was divided into two halves as shown in Fig. 2. In physiological situations is known that the growth of the ascending limb is slower than the fall in the descending limb. Earlier research showed that an increase in ventricular repolarization dispersion induces broad-based, symmetrically-shaped T-waves [15], and that abnormal increases in ventricular repolarization dispersion are linked to the risk of arrhythmia [10]. The relation between ventricular repolarization dispersion and cardiovascular risk, however, is still subject to debate in the scientific community. Furthermore, the spontaneous appearance of premature beats with specific ECG characteristics is also linked to the risk of arrhythmic events [33]. In this work, PVCs were observed in some recordings before the TdP event occurred during the first half of the T-wave. We extended the symmetry approach to dynamic features. The ω_{T21} ratio showed a trend towards 1 (Fig. 3), suggesting that the maximum ω_{T1}, corresponding to the first half of the T-wave, is increased and ω_{T2}, in the second half, is reduced. Although both the sensitivity and specificity values of this index are very high, the limits of their CIs are wide. This is due to the number of cases. As detailed below, a higher N would be required to reduce the amplitude of the CIs.

The linear velocity ratio has also been proposed as a risk marker that does not respond to the effects of beta-adrenergic blockers [34]. Our results, however, show that this index contributes to the separation of at-risk patients (+TdP) from subjects (−TdP) under the same treatment who did not suffer arrhythmia (See Table 2). One difference may arise from the velocity signal acquisition method. In the initial proposal, the derivative was performed with amplifiers with manual measurements. A higher time constant (10 ms) and analog filters were also used. In this study, signals were differentiated and digitally filtered. It is also possible that other differences arise from other ECG conditions.

The symmetry between the areas of both halves of the T-wave has also been used as a morphology descriptor [30,16]. Here, our method of normalizing the areas showed greater significance values than the standard indices from V5. The normalized areas would be less affected by noise since they included the information of all the leads. Thus, less information could be lost due to noise compared to a single lead. In addition, the use of PCA moves much of the noise to the residual components. However, the ratios reached similar results (See Table 2). Finally, the normalized areas helped enhance the distinction between the healthy population and patients with a history of TdP. In Fig. 4, although linear limits could be used with similar sensitivity/specificity results, the classification with quadratic limits highlighted the idea of symmetry. The small sample size in +TdP population requires further works to assess the final boundaries.

Currently, international regulatory agencies require a QTc index analysis for drug approval [4,5,35]. However, this approach has insufficient specificity. In fact, the at-risk patients studied here have suffered TdP events and only 67% had QTc values in the risk range (Section 3 and Table 1). Indices such as Tpe and QTc depend strongly on an accurate definition of the T_{END} point. The localization of T_{END} is much more difficult than T-wave peak, as the signal amplitude is low and the noise level can be higher than the signal itself [36]. Our method only uses the T-wave peak to differentiate the halves (Fig. 2). However, some authors stated that T-wave peak is determined by lead-specific projection of the vectorcardiographic T-wave loop and frequently differs lead to lead [37]. Thus, there may be burdened with additional

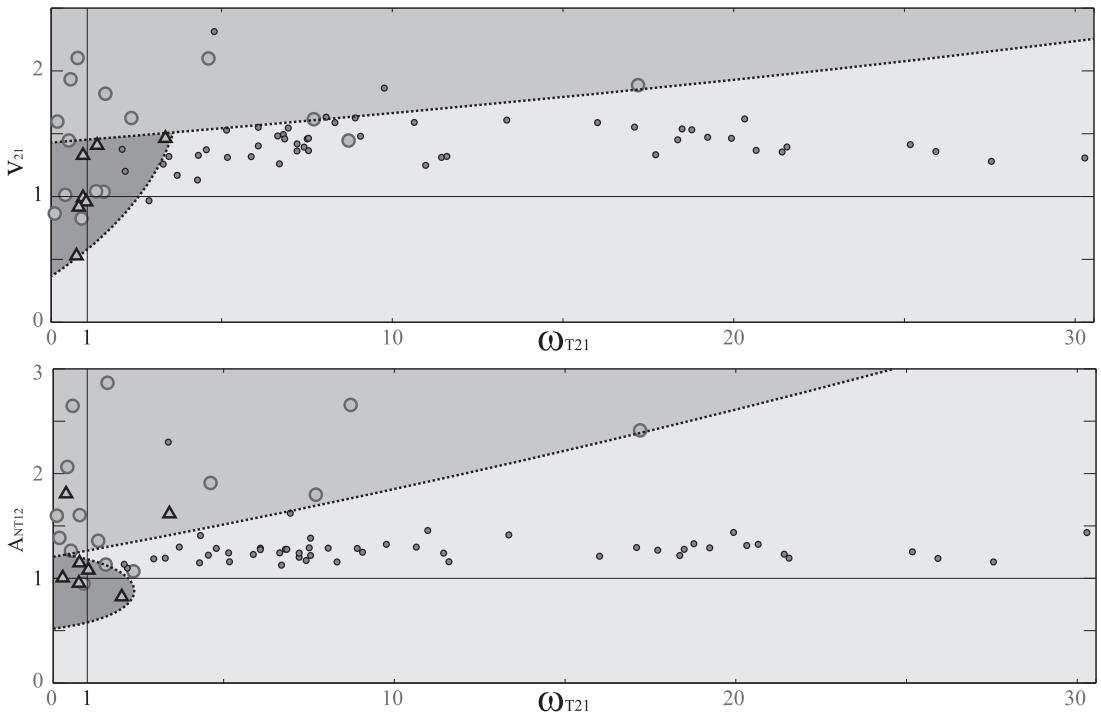

Fig. 4. Territorial maps for the three populations: '▲' for +TdP, 'o' for −TdP and • for Hs. Decision boundaries are determined using expanded five-dimensional quadratic polynomial functions.

uncertainty. The maximum velocities are several tens of milliseconds away the peak and would not depend on these values. This fact might explain the significant differences that were found in ω_{T2} but it was not possible to find in Tpe (Table 2). Nevertheless, although highly altered T-wave morphologies (such as biphasic T-waves) were not found in the analyzed databases, the definition of the halves could be affected in these cases. Subsequent studies should evaluate this question.

Finally, the new dynamic indices significantly improved the classification between +TdP and Hs populations compared to the standard QTc measurements. Moreover, it allowed us to observe a significant difference with respect to the subjects who, despite receiving the same drug, did not experience TdP. These indices are an interesting contribution to the challenge of discovering new risk markers for the development of safe drugs. Future research should be carried out with a greater sample size of at-risk patients, while observing how other conditions (such as gender, age or different ECG acquisition conditions) can affect the dynamics of ventricular repolarization.

5. Study limitations

The temporal analysis of the seven recorded episodes shows a strong tendency towards symmetry, as each TdP event approached. In addition, the differences in the risk profiles among the three populations were clearly reflected. Although our method is robust to noise and highly reproducible, since three different databases were used, the number of episodes registered is too low to allow definitive conclusions. In addition, the databases were recorded in different postural conditions (Holter and supine after a resting period), this could condition the results. Finally, the number of females were higher especially in the second database. We contemplated age and gender differences (Table 1) when computing the sensitivity and specificity of QTc. Despite differences in standard parameters of ventricular repolarization are understood [38], as far as we know, there are no well-established definitions of the influence of gender on the linear and angular velocities of the T-wave loop. So further research needs to be conducted to verify the results in different conditions and with a high level of statistical significance.

6. Conclusion

The findings of this study constitute a further sign of the great importance of the analyses of cardiac vector dynamics for risk assessment. The relation between the maximum angular velocities in both halves of the T-wave represents a valuable contribution to future research involving the development of risk markers for drug-induced arrhythmias. Combining this with linear velocity and area indices significantly enhanced the differences among the study populations. We trust that additional research on this approach will lead to the development of an efficacious tool that will surpass the effectiveness of existing measures and, undoubtedly, aid in the development of safe pharmacological therapies.

CRediT authorship contribution statement

Pablo Daniel Cruces: Conceptualization, Methodology, Software, Investigation, Formal analysis, Visualization, Writing – original draft, Writing – review & editing. **Alejandra Toscano:** Methodology, Software, Investigation, Formal analysis, Visualization. **Francisco Javier Alvarado Rodríguez:** Methodology, Software, Investigation, Formal analysis, Visualization. **Rebeca Romo-Vázquez:** Conceptualization, Investigation, Funding acquisition. **Pedro David Arini:** Conceptualization, Investigation, Writing – review & editing, Supervision, Funding acquisition, Project administration.

Declaration of competing interest

The authors declare that they have no known competing financial interests or personal relationships that could have appeared to influence the work reported in this paper.

Data availability

The authors do not have permission to share data.

Acknowledgments

This work was supported by CONICET, Argentina, under project PIP #112-20130100552CO and the Agencia MINCYT, Argentina, under project PICT 2145-2016, Argentina. The authors also acknowledge the National Science and Technology Council (CONACyT), Mexico, for the support received through the Fellowship CVU-746539. Finally, we thank Paul C. Kersey for copy-editing the manuscript.

References

[1] W.H. Organization, Noncommunicable diseases country profiles, 2014, www.who.int.
[2] J.P. Couderc, S. Kaab, M. Hinterseer, S. McNitt, X. Xia, A. Fossa, B.M. Beckmann, S. Polonsky, W. Zareba, Baseline values and sotalol-induced changes of ventricular repolarization duration, heterogeneity, and instability in patients with a history of drug-induced torsades de pointes, J. Clin. Pharmacol. 49 (2009) 6–16.
[3] A.J. Camm, Hopes and disappointments with antiarrhythmic drugs, Int. J. Cardiol. 237 (2017) 71–74.
[4] International Council on Harmonization, S7B the non-clinical evaluation of the potential for delayed ventricular repolarization (QT interval prolongation) by human pharmaceuticals, 2005, https://database.ich.org/sites/default/files/S7B_Guideline.pdf.
[5] International Council on Harmonization, E14 the clinical evaluation of QT/QTc interval prolongation and proarrhythmic potential for non-antiarrhythmic drugs, 2005, https://database.ich.org/sites/default/files/E14_Guideline.pdf.
[6] Y.G. Yap, A.J. Camm, Drug induced QT prolongation and torsades de pointes, Heart 89 (2003) 1363–1372.
[7] R.R. Shah, L.M. Hondeghem, Refining detection of drug induced proarrhythmia: QT interval and TRIaD, Heart Rhythm. 2 (2005) 758–772.
[8] N. Stockbridge, J. Morganroth, R.R. Shah, C. Garnett, Dealing with global safety issues: Was the response to QT-liability of non-cardiac drugs well coordinated? Drug Safety 36 (2013) 167–182.
[9] R.L. Woosley, K. Romero, C.W. Heise, T. Gallo, J. Tate, R.D. Woosley, S. Ward, Adverse drug event causality analysis (ADECA): A process for evaluating evidence and assigning drugs to risk categories for sudden death, Drug. Saf. 40 (6) (2017) 465–474.
[10] N.V. Arteyeva, Dispersion of ventricular repolarization: Temporal and spatial, World J. Cardiol. 12 (9) (2020) 437–449.
[11] L. Johannesen, J. Vicente, J.W. Mason, C. Sanabria, K. Waite-Labott, M. Hong, P. Guo, J. Lin, J.S. Sørensen, L. Galeotti, J. Florian, M. Ugander, N. Stockbridge, D.G. Strauss, Differentiating drug-induced multichannel block on the electrocardiogram: Randomized study of dofetilide, quinidine, ranolazine, and verapamil, Clin. Pharmacol. Ther. 96 (5) (2014) 549–558.
[12] J. Vicente, L. Johannesen, J.W. Mason, W.J. Crumb, E. Pueyo, N. Stockbridge, D.G. Strauss, Comprehensive t wave morphology assessment in a randomized clinical study of dofetilide, quinidine, ranolazine, and verapamil, J. Am. Heart Assoc. 4 (4) (2015) e001615.
[13] P.D. Cruces, D. Torkar, P.D. Arini, Biomarkers of pre-existing risk of torsade de pointes under sotalol treatment, J. Electrocardiol. 60 (2020) 177–183.
[14] T.P. Brennan, L. Tarassenko, Review of t-wave morphology-based biomarkers of ventricular repolarization using the surface electrocardiogram, Biomed. Signal Process. Control 7 (2012) 278–284.
[15] D. Di Bernardo, A. Murray, Explaining the T wave shape in the ECG, Nature 403 (2000) 40.
[16] M.P. Andersen, J.Q. Xue, C. Graff, J.K. Kanters, E. Toft, J.J. Struijk, New descriptors of T-wave morphology are independent of heart rate, J. Electrocardiol. 41 (2008) 557–561.
[17] P.D. Cruces, D. Torkar, P.D. Arini, Dynamic features of cardiac vector as alternative markers of drug-induced spatial dispersion, J. Pharmacol. Toxicol. Methods 104 (2020) 106894.
[18] P.D. Arini, R.A. Quinteiro, E.R. Valverde, G.C. Bertrán, M.O. Biagetti, Differential modulation of electrocardiographic indices of ventricular repolarization dispersion depending on the site of pacing during premature stimulation, J. Cardiovasc. Electrophysiol. 12 (2001) 36–42.
[19] M. Ghannam, K.C. Siontis, M.H. Kim, H. Cochet, P. Jais, M.J. Eng, A. Attili, G. Sharaf-Dabbagh, R. Latchamsetty, K. Jongnarangsin, F. Morady, F. Bogun, Risk stratification in patients with frequent premature ventricular complexes in the absence of known heart disease, Heart Rhythm 17 (3) (2020) 423–430.
[20] Telemetric and Holter ECG Warehouse, Recorded "Torsades de Pointes" Event Database, http://thew-project.org/Database/E-OTH-12-0006-009.html.
[21] Telemetric and Holter ECG Warehouse, Cardiac Patients with and without a History of Drug-induced Torsades de Pointes, http://thew-project.org/Database/E-OTH-12-0068-010.html.
[22] R. Bousseljot, D. Kreiseler, A. Schnabel, Nutzung der EKG-signaldatenbank CARDIODAT der PTB über das internet, Biomed. Tech. 1 (317) (1995).
[23] A.L. Goldberger, L.A.N. Amaral, L. Glass, J.M. Hausdorff, P.C. Ivanov, R.G. Mark, J.E. Mietus, G.B. Moody, C.-K. Peng, H.E. Stanley, PhysioBank, PhysioToolkit, and PhysioNet: Components of a new research resource for complex physiologic signals, Circulation 101 (23) (2000) e215–e220.
[24] P.D. Cruces, P.D. Arini, Quaternion-based study of angular velocity of the cardiac vector during myocardial ischaemia, Int. J. Cardiol. 248 (2017) 57–63.
[25] A.J. Demski, M. Llamedo Soria, Ecg-kit: A Matlab toolbox for cardiovascular signal processing, J. Open Res. Softw. 4 (1) (2016) e8.
[26] E. Frank, An accurate, clinically practical system for spatial vectorcardiography, Circulation 13 (1956) 737–749.
[27] J.A. Kors, G. Van Herpen, J.H. Van Bemmel, Reconstruction of the frank vectorcardiogram from standard electrocardiographic leads: Diagnostic comparison of different methods, Eur. Heart J. 11 (1990) 1083–1092.
[28] B. Barsky (Ed.), Rethinking Quaternions. Theory and Computation, Morgan & Claypool, California, 2010, pp. 95–100.
[29] A.S. Poznyak, Modelado Matemático de los Sistemas Mecánicos, Eléctricos y Electromecánicos, Pearson, 2005, pp. 73–83, ch. 2.
[30] M. Merri, J. Benhorin, M. Alberti, E. Locati, A.J. Moss, Electrocardiographic quantitation of ventricular repolarization, Circulation 80 (1989) 1301–1308.
[31] R. Panikkath, K. Reinier, A. Uy-Evanado, C. Teodorescu, J. Hattenhauer, R. Mariani, K. Gunson, J. Jui, S.S. Chugh, Prolonged tpeak-to-tend interval on the resting ECG is associated with increased risk of sudden cardiac death, Circ. Arrhythm. Electrophysiol. 4 (4) (2011) 441–447.
[32] P.D. Cruces, M. Llamedo Soria, P.D. Arini, Velocity tracking of cardiac vector loops to identify signs of stress-induced ischaemia, Med. Biol. Eng. Comput. 60 (5) (2022) 1313–1321.
[33] T. Yamada, Twelve-lead electrocardiographic localization of idiopathic premature ventricular contraction origins, J. Cardiovasc. Electrophysiol. 30 (11) (2019) 2603–2617.
[34] A. Sasaki, A. Takimiya, T. Arai, Y. Song, S. Nakajima, K. Muto, C. Ibukiyama, Abnormalities of t waves in effort angina pectoris patients at rest evaluated by spatial velocity electrocardiogram, Jpn. Heart J. 37 (1996) 879–889.
[35] M. Li, L.G. Ramos, Drug-induced QT prolongation and torsades de pointes, Pharmacovigil. Forum 42 (7) (2017) 473–477.
[36] J.P. Martínez, R. Almeida, S. Olmos, A.P. Rocha, P. Laguna, A wavelet-based ECG delineatior: Evaluation on standard databases, IEEE Trans. Biomed. Eng. 51 (4) (2004) 570–581.
[37] M. Malik, H.V. Huikuri, F. Lombardi, G. Schmidt, R.L. Verrier, M. Zabel, Is the tpeak-tend interval as a measure of repolarization heterogeneity dead or just seriously wounded? Heart Rhythm. 16 (6) (2019) 952–953.
[38] H. Bidoggia, J.P. Maciel, N. Capalozza, S. Mosca, E.J. Blaksley, E. Valverde, G. Bertran, P. Arini, M.O. Biagetti, R.A. Quinteiro, Sex-dependent electrocardiographic pattern of cardiac repolarization, Am. Heart J. 140 (3) (2000) 430–436.